International Journal of Applied Engineering Research ISSN 0973-4562 Volume 12, Number 15 (2017) pp. 5067-5072

The Influence of Gravity Shear Ratio on the Behaviour of Reinforced Concrete Slab-Column Connections with Shear Reinforcement

Faimun[1], Asdam Tambusay[2,*] and Priyo Suprobo[3]

[1,2,3]*Department of Civil Engineering, Sepuluh Nopember Institute of Technology, Indonesia.*

[2]*ORCID: 0000-0002-0314-5104*

Abstract

A numerical analysis has been undertaken to study the behaviour of slab-column connections under high gravity shear ratio. A half-scale reinforced concrete slab-column connection with shear reinforcement was modelled in finite element (FE) tool called ABAQUS. The specimen was subjected to combined constant gravity and reversed cyclic lateral load. Prior to executing the numerical modelling of the specimen, one specimen following the model similar to the previous study was first modelled as a means of verification purpose. Upon this phase, further analysis was then performed by merely modifying the magnitude of gravity shear ratio being applied to the specimen with the value of 0.4 specified as the maximum allowable gravity shear ratio for slab-column connection. In addition, the cyclic lateral load was then given afterwards using displacement control method. It is shown that the influence of high gravity shear ratio clearly reduces the lateral drift capacity. The result also resembles the trend of drift capacity versus gravity shear ratio when being compared to the drift limits from the design specification and prior studies.

Keywords: Reinforced concrete, slab-column connection, shear reinforcement, gravity shear ratio, cyclic lateral load, numerical analysis.

INTRODUCTION

Reinforced concrete structures featuring slabs and directly supported by the columns without the use of beam member are referred to as slab-column frames or flat plate structures [1]. This type of systems offers economic efficiency due to the absence of the beams, easy formwork system and rapid construction [2]. In addition, larger opening space with reduced story height is one of the advantages of this system, allowing to increase the number of floors in strict restriction of building height [3]. Slab-column frames also offer the unique benefit of improving fire-resistant due to the absence of sharp corners; hence there is less danger of the concrete spalling when the reinforcement being exposed to the fire [4].

The performance of flat slab structures under seismic load has been majorly reported in the previous studies considering their behaviour as exterior and interior of slab-column connections. The results showed that brittle punching shear occurred in the critical zone was typically caused by the combination of direct shear stress due to gravity load and the unbalanced moment formed as eccentric shear stress. Prior research conducted by Robertson *et al.* [5–6] also reported that the gravity shear was one of the significant factors which triggered a setback of drift capacity of the connection [6]. It was also shown that initial cracks were developed and progressed alongside the critical area of slab adjacent to the column face during the application of gravity load [7].

An attempt had also been undertaken to improve the punching shear capacity of slab-column connections under gravity load. This was done by giving a certain amount of slab shear reinforcement. The reinforcement was preferably designed to be continuous at the joint to alleviate the adverse effect of the structure failure [8]. Given the facts of punching shear failure

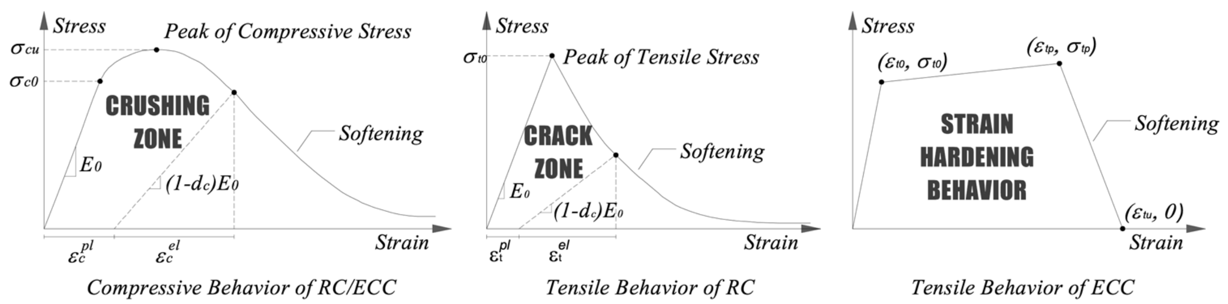

Figure 1: Parameters of concrete damage plasticity model.

*asdam.tambusay13@mhs.ce.its.ac.id (corresponding author)

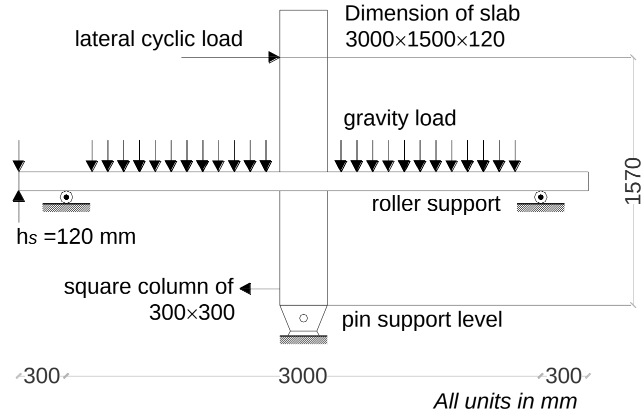

Figure 2: Schematic geometry of test specimen [9].

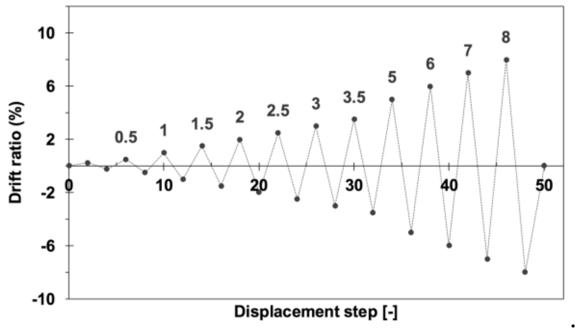

Figure 4: Reversed cyclic lateral displacement protocol

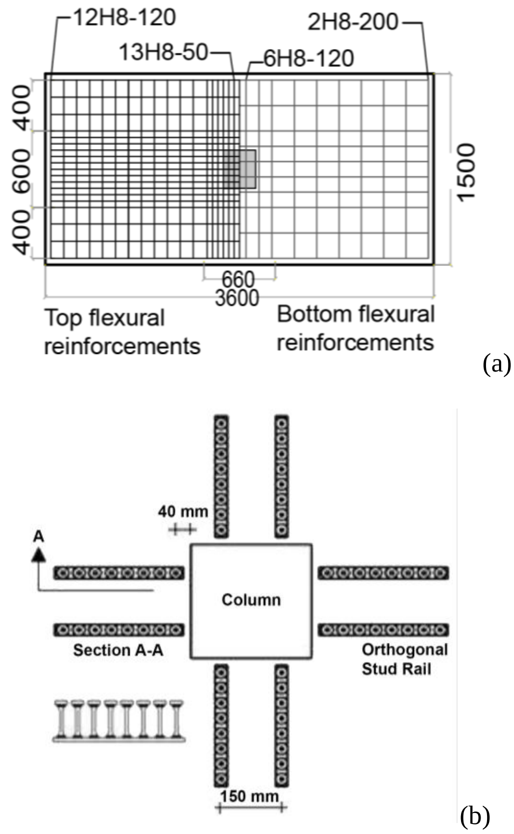

Figure 3: Reinforcement layouts of the test specimen: (a) longitudinal reinforcement, (b) stud rail layout [9].

due to the influence of gravity shear ratio, it is of importance to provide improved insights with regard to this situation. Therefore, this paper aims to study the influence of high gravity shear ratio in a typical reinforced concrete slab-column connection provided by shear reinforcement. Despite being simulated in the numerical environment; the modelling technique can be used to carry out a further analysis with varying parameters being used in the model.

RESEARCH SIGNIFICANCE

The majority of the investigations on slab-column connection was merely conducted in laboratory experimental-based. It is, therefore, a necessity to offer the different approach in a way the analysis can also be performed to understand the behaviour of such structure. Fewer studies of this type of structure also sum up the need to provide more insights into the behaviour, particularly the influence of high gravity shear ratio as the primary objective of this present work. To ensure whether or not the constitutive modelling adopted in the simulation is reasonably accurate, typical specimen from the previous work conducted by Gunadi *et al.* [9] is first modelled.

MODELLING TECHNIQUE

In this study, the finite element analysis of slab-column connections was performed through the use of available commercial nonlinear software called ABAQUS. The solid continuum of the C3D8R element was adopted for concrete material to represent the eight-node solid brick element. Each node has three degrees of freedom in the form of translation in the direction of x, y, and z. In addition, C3D8R with reduced integration was also considered as it follows a lower-order integration to form the element stiffness. The normal plasticity model was selected for reinforcement bar by using T3D2 truss element. In T3D2, the element is assumed as a 3D model having two degrees of freedom. This element was created using 3D wire instead of the solid element. This was done to eliminate any complication during the iteration process due to the imperfect nodal encounter between concrete and reinforcing steel thereby causing the heavy computational load. As the wire was used, embedded element constraint was also adopted to represent the contact between the concrete and the reinforcing steel. Once the reinforcing steel has been embedded, the transitional degree of freedom will then be eliminated by all means [10].

To account the nonlinearity of quasi-brittle such as concrete, the plasticity-based model referred to as concrete damage plasticity model (CDPM) was used in this study. CDPM works by assuming that the failure mechanisms consist of tensile cracking and compressive crushing [11]. The evolution of the yield (or failure) surface is controlled by two hardening variables $\tilde{\varepsilon}_t^{pl}$ and $\tilde{\varepsilon}_c^{pl}$ which they are associated to failure mechanisms under tension and compression respectively [12]. If E_0 is the initial (undamaged) elastic stiffness of the material, the stress-strain relations under uniaxial tension and compression loading are expressed in Equation (1).

$$\sigma_t = (1 - d_t) E_0 \left(\varepsilon_t - \tilde{\varepsilon}_t^{pl}\right) \qquad (1a)$$

$$\sigma_c = (1 - d_c) E_0 \left(\varepsilon_c - \tilde{\varepsilon}_c^{pl}\right) \qquad (1b)$$

The fundamental relationships of stress and strain under compression and tension are also shown in **Figure 1**. For more detailed information regarding the CDPM equations, the readers are referred to References 11 and 12.

EXPERIMENTAL AND FE PROGRAMME

A. Experimental programme

An experimental investigation conducted by Gunadi *et al*. [9] was readdressed herein as a means for verification purposes to the finite element analysis. Only one specimen was used to perform the analysis. According to the detail of specimen being used in their work, the test specimen was a half-scale interior slab-column connection representation of typical flat plate structure. The shear reinforcement in the form of orthogonal stud rail as stated in design specification [13] was provided in the slab. The specimen had a geometry with the length of 3.0 m, the width of 1.5 m, and the slab thickness of 120 mm. The schematic geometry of specimen is shown in **Figure 2**, with the material properties of the specimen summarised in **Table 1**.

In accordance with design specification [8], the flexural reinforcement must be designed relatively dense around the critical region, preferably in the effective width of the slab with the distance of approximately $c + 3h$, where c is the column width, and h is the slab thickness. It is of importance to take this into account as the unbalanced moment transferred into flexure is encountered alongside this region. In this particular study, the top and bottom reinforcement ratio of slab within the effective width was designed to be 0.9% and 0.4% respectively. Details of slab longitudinal and shear reinforcement layouts are shown in **Figure 3**.

The specimen was subjected to constant gravity load using concrete blocks placed underneath the slab. These concrete blocks were hung by steel hooks which were attached to the top flexural reinforcement prior to concrete casting. The accumulation of weight in all concrete blocks was similar to gravity shear ratio of 0.1. In a later sequence, the lateral cyclic load was then applied with the aid of hydraulic actuator placed horizontally to the column tip. The cyclic load was

Table 1: Material properties of test specimen.

Designation	Diameter (mm)	f_y (MPa)
Longitudinal rebar of column	13.84	390.74
Flexural reinforcement of slab	7.96	321.5
Column stirrup	5.94	354.77
Stud Rail	7.68	534.3

Table 2: Initial gravity shear ratio.

Specimen	Shear force, V_g (kN)	Section area, A_c (10^4 mm^2)	Shear stress, v_{ug} (MPa)	Nominal stress, v_n (MPa)	Shear ratio, v_{ug}/v_n
1	65.21	28.45	0.23	2.26	0.10
2	255.5	28.45	0.90	2.26	0.40

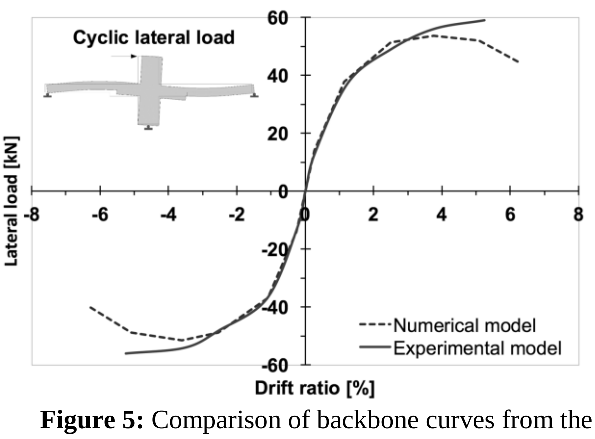

Figure 5: Comparison of backbone curves from the experimental and numerical results.

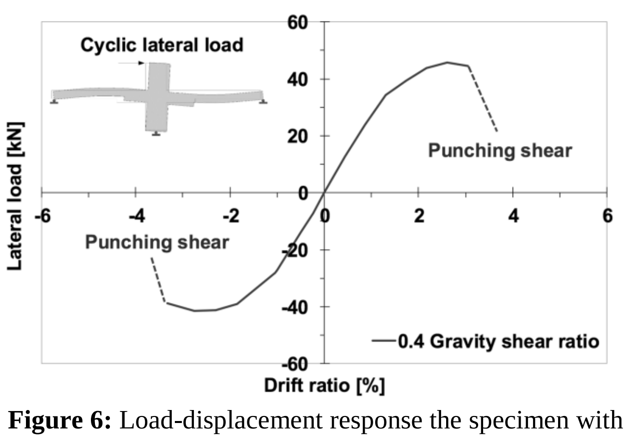

Figure 6: Load-displacement response the specimen with 0.4 gravity shear ratio.

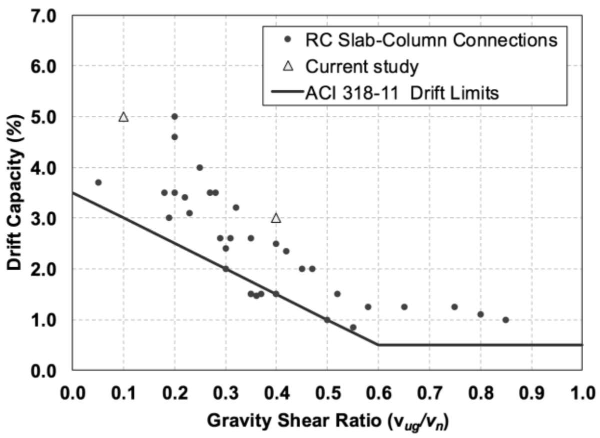

Figure 7: Gravity shear ratio versus connection drift capacity.

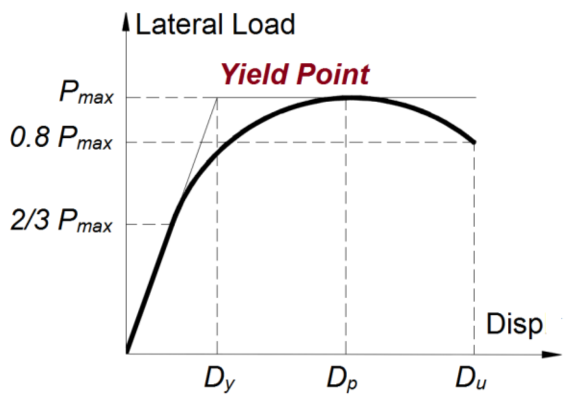

Figure 8: Illustration of ductility definition.

Table 3: Displacement ductility.

Specimen	Drift ratio (%)			Ductility	
	Yield point	Maximum point	Ultimate point	Ratio of maximum displacement over yield displacement	Ratio of ultimate displacement over yield displacement
1	1.85	4.0	6.16	2.67	3.32
2	1.55	3.01	3.85	1.94	2.48

given in the form of displacement control starting with a low rate to evade the nonlinearity issue during the initial condition.

B. Finite element programme

A numerical analysis was performed by adopting the similar specimen from the experimental work by Gunadi *et al.* [9]. This was done to deliver direct validation with regard to the trend of the backbone curve. The numerical simulation was performed by considering the variety of parameters such as mesh configuration, type of element, boundary conditions and so on, which mostly have been mentioned in the previous section.

In the modelling, self-weight of the specimen was defined as density. ABAQUS automatically calculated the weight of the specimen by the density of material multiplied by its volume after assigning the gravitational acceleration in the load module. Superimposed dead load was given in the form of pressure load, while the cyclic lateral load was given using displacement control featured in amplitude module. Detail of the displacement routine applied to the specimen is shown in **Figure 4**.

With regard to the numerical result, **Figure 5** presents the comparison of backbone curve obtained from the experimental and numerical investigation. It is shown that both curves have similar trend up to drift ratio of 4% in terms of lateral load and stiffness. A discernible deviation occurs at 5% drift ratio. From what is encountered in **Figure 5**, it can be said that the finite element analysis has been run with the proper modelling technique.

Following the triumph of numerical validation, a further finite element analysis was undertaken by modifying the magnitude of gravity load. The further model was subjected to high gravity shear ratio with the value being applied 0.4 (for more detailed information see **Table 2**). Basically, the gravity shear ratio is defined as the ratio of direct shear stress due to gravity load over the nominal shear stress provided by concrete and steel (if any). The equation of gravity shear ratio is relatively straightforward and can be written as v_{ug} /v_n.

RESULTS AND DISCUSSION

A. Load-displacement relationship

Figure 6 shows the relationship of load versus lateral displacement of the specimen subjected to 0.4 gravity shear ratio. It is evident from the figure that the specimen undergoes significant shortcoming in lateral drift capacity. The influence of high gravity load can reduce the lateral drift capacity up to 60% if compared to the result of 0.1 gravity shear ratio. It is also shown that the peak lateral load is only achieved at 2.61% drift level, meaning this value is not even satisfying the minimum requirement of earthquake proof and resistant structure as specified by ACI Committee [14]. It is worth to mention when the load is in the post-peak response, the convergence issue is present in the numerical modelling, triggering the abortion as the structure does not withstand the applied load any longer.

B. Connection drift capacity

As mentioned in the previous subsection, the influence of gravity shear ratio does show the significant reduction in the connection drift capacity. This can be confirmed by the test summary of drift capacity reported in the prior studies concerning the effect of gravity shear ratio. **Figure 7** shows the experimental results of the past research using shear reinforcement, with the results from this present work being plotted as well.

From what is seen in the figure, the evaluation regarding gravity shear ratio has now been studied with varying ratio up to 0.85. The data trend confirms that there is indeed the reduction in lateral drift capacity as the gravity shear ratio increases. With regard to the numerical results, it is also apparent that the plots show reasonable agreement with prior studies as well as the drift limits specified by the ACI Committee [13]. Through this evaluation, it can be said that the results seem to indicate the important role of gravity shear ratio in influencing the drift capacity and punching failure.

C. Ductility

Displacement ductility (μ) is defined as the ratio of displacement at ultimate load (D_u) or peak displacement (D_p) over the displacement at the first yield point (D_y). In relation to this present work, the displacement ductility of each specimen is calculated based on the backbone curve. Since the yield point in slabs sometimes is well not defined due to the punching failure prior to significant yielding of slab reinforcement, an arbitrary procedure must be taken in order to define a proper yield drift [5]. The procedure of determining displacement ductility is illustrated in **Figure 8** (only the curve in the positive direction is displayed). **Table 3** presents the results of displacement ductility of the specimens with the gravity shear ratio of 0.1 and 0.4. It is shown that the ductility provided by the specimen with low gravity shear ratio is much higher than that of the specimen with low gravity shear ratio.

CONCLUSION

Punching shear failure is a brittle phenomenon which can occur with no prior warning. It is thus of critical importance to provide insights of what factor triggers the above condition such as gravity shear effect. From this limited investigation the following conclusion can be drawn:

1. It has been shown that under low gravity shear ratio, the specimen of slab-column connection can withstand the load beyond the drift ratio of 6%. This can be associated with the ductile plateau upon the initial yielding condition.
2. Despite using the shear reinforcement, the specimen subjected to high gravity shear ratio exhibits a significant reduction in terms of lateral drift capacity.
3. Increasing the gravity shear ratio also considerably reduced the displacement ductility as this factor is related to the connection drift capacity.
4. In terms of overall results, it has been shown that the numerical results show a reasonable agreement with the results obtained from the experimental work.

ACKNOWLEDGEMENTS

The authors wish to acknowledge all the supports provided by the Department of Civil Engineering at Sepuluh Nopember Institute of Technology.

REFERENCES

[1] Cheng M. Y., “Punching shear strength and deformation capacity of fiber reinforced concrete slab-column connections under earthquake loading,” *PhD Dissertation*, Al-Rasheed Civil Engineering Department, the University of Michigan, United States, 2009.

[2] Changsoon, R., Kang, T. H. K., Shin, M., and Yoon, J. B., “Gravity and lateral load-carrying capacities of reinforced concrete flat plate systems,” *ACI Structural Journal*, vol. 111, no. 4, pp. 753–764, 2014.

[3] Matzke, E. M., Lequesne, R. D.m Parra-Montesinos, G. J. and Shield, C. K., “Behavior of biaxially loaded slab-column connections with shear stud,” *ACI Structural Journal*, vol. 112, no. 3, pp. 335–346, 2015.

[4] Erberik, M. A., and Elnashai, A. S., “Fragility analysis of flat-slab structures,” *Engineering Structures*, vol. 26, pp. 937–948, 2004.

[5] Robertson, I., and Durrani, A. J., “Gravity load effect on seismic behavior of exterior slab-column connections,” *ACI Structural Journal*, vol. 88, no. 3, pp. 255–267, 1991.

[6] Robertson, I., and Durrani, A. J., “Gravity load effect on seismic behavior of interior slab-column connections,” *ACI Structural Journal*, vol. 89, no. 1, 37–45, 1993.

[7] Robertson, I., Kawai, T., Lee, J., Enomoto, B., “Cyclic testing of slab-column connections with shear reinforcement,” *ACI Structural Journal*, vol. 99, no. 5, pp. 605–613, 2002.

[8] Robertson, I., and Johnson, G., “Cyclic lateral loading of nonductile slab-column connections,” *ACI Structural Journal*, vol. 103, no. 3, pp. 356–364, 2006.

[9] Gunadi, R., Budiono, B., Imran, I., and Sofwan, A., “Peningkatan perilaku hubungan pelat-kolom terhadap beban lateral siklis dengan menggunakan detail tulangan geser baru,” *Prosiding Konferensi Nasional Pascasarjana Teknik Sipil (KNPTS)*, pp. 66–76, 2012.

[10] Tambusay, A., Suprobo, P., Faimun, & Amiruddin, A. A., “Finite element modelling of a reinforced concrete and slab-column connection under cyclic lateral load,” *International Journal of Applied Engineering*

Research ISSN 0973–4562, vol. 12, no. 9, pp. 1987–1993, 2017.

[11] Tambusay, A., Suprobo, P., Faimun, & Amiruddin, A. A., “Finite element analysis on the behaviour of slab-column connections using PVA-ECC material,” *Jurnal Teknologi (Science and Engineering)*, vol. 79, no. 5, pp. 23–32, 2017.

[12] ABAQUS, “Abaqus analysis user’s manual version 6.14,” *Dassault System*, 2014.

[13] ACI Committee 318, “building code requirements for structural concrete (ACI 318-11) and commentary,” American Concrete Institute, 2011.

[14] ACI Committee 374, “Acceptance criteria for moment frames based on structural testing and commentary (ACI 374.1-05),” American Concrete Institute, 2005.